BASIC TECHNIQUES OF SURFACE PHYSICS

Surface Analysis with Temperature Programmed Desorption and Low-Energy Electron Diffraction

---

Versuch Nr. 89

F-Praktikum in den Bachelor- und Masterstudiengängen, SS2017

Physik Department

Lehrstuhl E20, Raum 205

Contacts: Dr. Y.-Q. Zhang, Dr. T. Lin and Dr. habil. F. Allegretti

---

1 Introduction

Surface science is a wide and interdisciplinary field of research that deals with the physical and chemical processes occurring at the interface between two physical phases, e.g. the solid-gas and the solid-vacuum interface. It emerged as an independent discipline in the early 1960s, thanks to the advances in ultra-high vacuum (UHV) technology, in the understanding of atom-solid and electron-solid interactions, and in the production of high-quality single-crystal surfaces. The adsorption and ordering of molecular species at atomically well-defined surfaces is a central topic in surface science, which underpins the microscopic understanding of surface chemical reactions and of the processes governing heterogeneous catalysis. This F-Praktikum experiment aims to familiarize the students with fundamental concepts of molecular adsorption and desorption phenomena by exploiting two important techniques for the characterization of surfaces, namely **Temperature Programmed Desorption** (**TPD**) and **Low-Energy Electron Diffraction** (**LEED**). The latter probes the long-range ordering, symmetry and periodicity of an adsorbed molecular layer relative to the underlying surface, the former monitors the desorption of the molecules and/or reaction fragments from the surface when the sample temperature is increased continuously and thus yields important information on the molecule-surface interaction.

The experiment will introduce the students to the principles and basic methodology of TPD and LEED. The exemplary case of the adsorption (and desorption) of carbon monoxide (CO) on the (0001) surface of a Ru single crystal under UHV conditions will be illustrated in detail. The technical basis and scientific content of the experiment include:

- basics of ultra-high vacuum technology
- basics of surface preparation protocols
- computer control of the TPD measurements
- TPD data analysis via computer software
- acquisition of electron diffraction patterns and determination of surface order by reciprocal-space analysis
- monitoring of electron-beam induced damage of molecular species

The experimental session will typically last about five hours. Subsequently, the drafting of a short scientific report (in English) within few weeks from the experiment will be followed by a 30 min. colloquium.

2 Adsorption on surfaces

To start with, we briefly define some fundamental concepts, which are important to describe and categorize adsorption phenomena on solid surfaces.
Adsorption is a process by which foreign species, atoms or molecules, are trapped on a substrate surface and stick (i.e., bind) to it upon condensation from the gas phase. The energy released in this process is called *energy of adsorption* or *binding energy*, E_b. The term *substrate* refers to the solid surface onto which adsorption occurs, while *adsorbate* is used to indicate the species that are adsorbed onto the substrate (Fig. 1). Adsorption can be associative (if a particle or molecule is adsorbed as a single entity) or dissociative (if the particle or molecule is dissociated upon adsorption); moreover adsorption processes may be reversible or irreversible. The reverse process, leading to the removal of adsorbed species from the surface, is called *desorption*. It can be induced by heat (thermal desorption), by electrons (electron stimulated desorption), or by photons or ions (photon or ion stimulated desorption).

2.1 Types of adsorption

The adsorption of atoms or molecules on solid surfaces is governed by the same fundamental forces that are treated in the quantum-mechanical theory of chemical bonding. In particular, depending on the strength of the adsorbate-substrate interaction, a clear-cut distinction between two limiting cases can be made:

Physisorption
Physical adsorption (= physisorption) is driven by weak, long-range van der Waals interactions with the surface; no chemical bonds are established and the perturbation of the electronic states of the adsorbate is generally marginal. The adsorption energy E_b is small, typically ≤ 0.3 eV per atom or molecule (i.e., per mole, ≤ 30 kJ/mol). Physisorption is not strongly surface-specific: it can take place – in principle – for all molecules on any surface provided that the temperature is low enough. As a consequence, formation of multilayers (condensates) is always possible at sufficiently low temperatures. Rare gases on metal surfaces are a characteristic example of physisorbed systems, whereby temperatures lower than 30 K are needed for the adsorption of Ar and lower than 80 K for Xe.

Typical physisorption potentials display a trend as a function of the adsorbate-to-substrate distance similar to those shown in Fig. 2a. They are characterized, in general, by a low binding energy (depth of the potential well) of ~ 0.25 eV or less, and by a

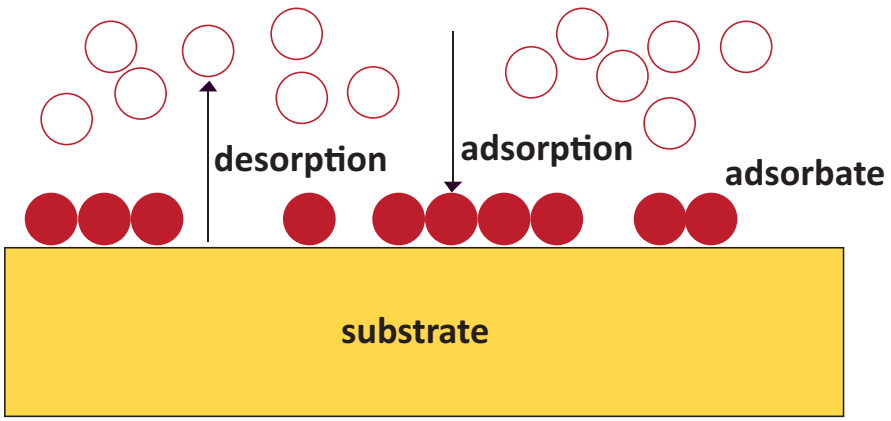

Figure 1: Schematic illustration of adsorption onto, and desorption from, a substrate surface. The spheres representing atoms of the adsorbate are filled in red, while gas-phase atoms are coloured in white.

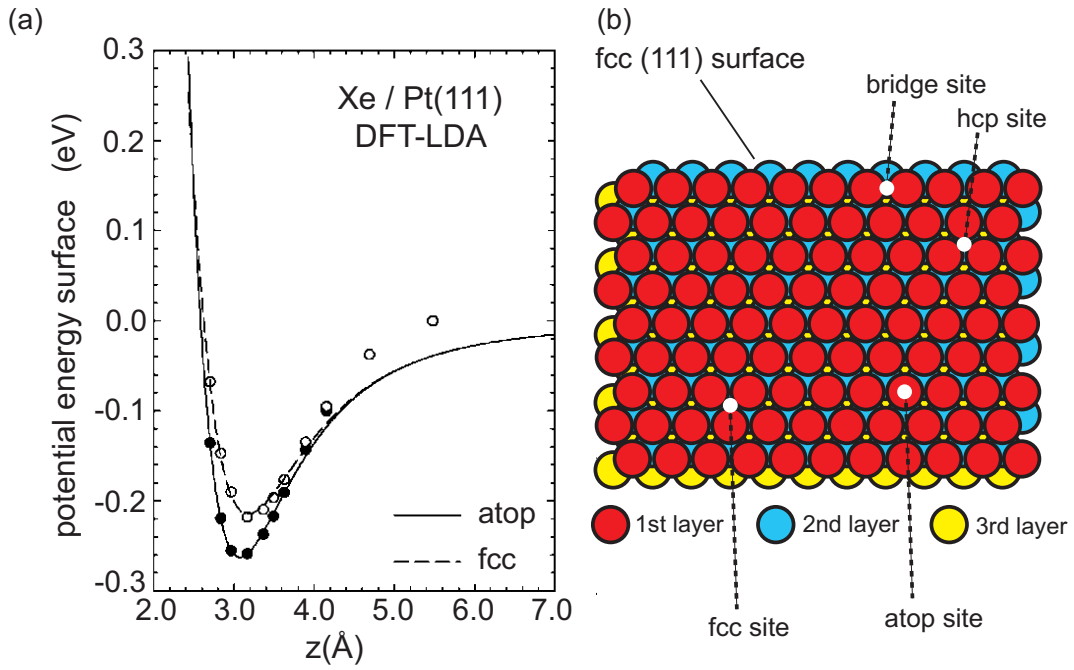

Figure 2: (a) Calculated potential energy for Xe physisorbed on Pt(111) for the atop and fcc sites, see also panel (b), as a function of the distance from the surface. Adapted from Ref. [1]. Density functional theory (DFT) calculations within the local density approximation (LDA) were performed by Da Silva *et al.* [1]. (b) Structure of the close-packed (111) surface of a face-centred cubic (fcc) crystal, such as Pt(111) or Rh(111), illustrating different high symmetry sites for adsorption. Specifically, the atop (above a first layer atom), hcp (above a second layer atom) and fcc (above a third layer atom) sites are highlighted.

relatively large equilibrium separation (distance between the potential minimum and the surface) of $3 - 7$ Å.

Chemisorption

Chemical adsorption (= chemisorption) entails the formation of a chemical bond between the adsorbate and the surface, e.g. *via* transfer of electrons and/or hybridization of molecular orbitals leading to formation of covalent bonds. In most cases the adsorption energy per particle is substantially larger than 0.3 eV, typically ≥ 1 eV/particle (or ≥ 100 kJ/mol). Chemisorption on reactive surfaces is often dissociative; it may also be irreversible, resulting in desorption of molecular fragments upon heating. Activation barriers can be involved, and chemisorbates form typically only a single layer in direct contact with the surface atoms of the substrate. Moreover, specific binding sites may be favoured because of the highly corrugated landscape of the surface potential. For instance, CO chemisorbs on Rh(111) with the intact CO molecules positioned exclusively in atop positions (i.e., on top of a Rh surface atom) at low coverage [2]. However, at the saturation coverage upon completion of a more densely packed layer, the CO molecules occupy both atop and threefold hollow sites (namely, the fcc and hcp sites illustrated in Fig.2b) [2].

Oxygen (O_2) and hydrogen (H_2) molecules usually result in dissociative chemisorption on transition metal surfaces (such as Rh, Pd and Ru surfaces) at room temperature (300 K), forming a saturation layer of atomic O or H, respectively. As the the chemisorption potential of the individual atomic species follows the trend of Fig. 3a, the combination with the shallower physisorption potential for the intact molecule, e.g. H_2 on a metal substrate, leads to a qualitative shape as shown in Fig. 3b (continuous line). A molecule approaching the surface will initially follow the physisorption potential curve,

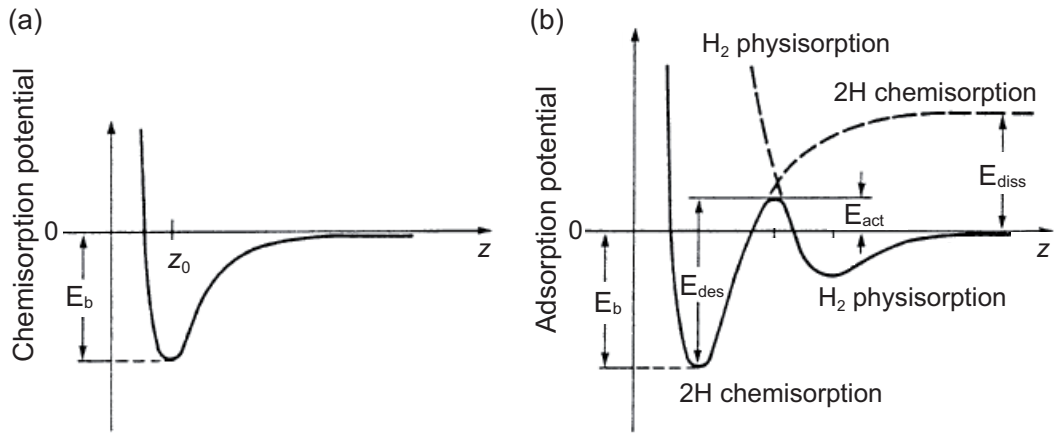

Figure 3: (a) Qualitative trend of the chemisorption potential as a function of the distance z of an adsorbed atom or molecule from the underlying solid surface. The equilibrium distance z_0 is typically smaller than 3 Å and the binding energy E_b of the order of 1 eV. (b) Combination of chemisorption and physisorption potentials illustrated qualitatively for the case of dissociative adsorption of hydrogen (H_2) on a metal surface. E_{diss} represents the dissociation energy of H_2 in the gas phase, E_{act} the activation energy for adsorption, E_b the binding energy in the chemisorption state with two chemisorbed H atoms, and E_{des} the activation energy for recombinative desorption of 2H. Adapted from Ref. [3].

but if it possesses enough kinetic energy to overcome the activation barrier E_{act} when entering the repulsive region of the curve, it will then preferentially follow the chemisorption potential curve and will be dissociated into two atoms, which adsorb on the surface forming two chemisorption bonds with the metal. The resulting adsorption energy is E_b, whereas associative desorption from the surface ($H + H \rightarrow H_2$ for the case of Fig. 3b) requires an energy E_{des}.

In practice, the distinction between chemisorption and physisorption is not always sharp, and especially for large molecules, the interplay of different and competing interactions (including chemical and van der Waals interactions with the substrate, but also adsorbate-adsorbate, i.e. intramolecular, interactions) *via* specific functional groups can lead to variegated adsorption scenarios.

2.2 Adsorption order

The adsorption order is another useful concept for the classification and description of adsorption and desorption processes. In particular, for the examples mentioned above first- and second-order adsorption are important:

- **First-order adsorption**
  One particle from the gas phase yields one particle of the adsorbate, i.e., the impinging particles are molecules that do not dissociate upon adsorption. The reverse process is first-order desorption.
  Examples: CO/Nickel (CO chemisorbs on Ni surfaces molecularly, $E_b \sim 120$ kJ/mol); Ar/Ruthenium (Ar physisorbs on Ru with $E_b \sim 10$ kJ/mol).

- **Second-order adsorption**
  A molecule dissociates upon adsorption. One particle in the gas phase yields two particles on the surface. The reverse process is called second-order (or associative) desorption.
  Example: H_2/Nickel (H_2 dissociates into two H atoms on Ni, $E_b \sim 90$ kJ/mol).

3 Experimental techniques

We now briefly describe the two principal techniques that will be used in this F-Praktikum experiment to characterize the adsorption of gas molecules, CO, on a metal surface, Ru(0001).

3.1 Temperature Programmed Desorption

Temperature Programmed Desorption (TPD) is a powerful and well-established technique for surface studies. It is based on the incremental heating of an adsorbate-covered substrate which induces desorption of atoms, molecules and/or molecular fragments from the surface. As such, it provides crucial information on the strength of the interfacial bonding and interactions between the adsorbate and the substrate along with the occurrence of thermally activated chemical reactions. Notably, it can also give access to important kinetic and thermodynamic parameters of the desorption process.

In a typical TPD experiment, the sample is heated at a constant rate $\beta = dT/dt$, and the temperature T thus increases linearly with the time t: $T(t) = \beta \cdot (t - t_0) + T_0$. When an appropriate temperature is reached, the thermal energy provided to an adsorbate species may become sufficient to make it desorb from the surface, thus yielding a peak in the desorption rate. The counting rate of the desorbing species is monitored as a function of temperature (or time) by means of a Quadrupole Mass Spectrometer (QMS) positioned in front of the sample surface at close distance.

In the QMS the incoming molecules or atoms are firstly ionized and then filtered according to their mass-to-charge ratio (m/e). As shown in Fig. 4a, the QMS typically consists of an electron impact ionizer (where bombardment by electrons from a hot filament is exploited to generate a current of positive gas ions), an ion accelerator and mass filter, and an ion detector. The filtering action is realized through the quadrupole electric field generated by an array of four parallel metal rods, which are pairwise biased by an AC radio frequency voltage with a DC offset applied [3]. The general working principle can be understood qualitatively in the following way. Along the x direction, light ions (i.e., low m/e ratio) can follow the AC voltage and oscillate with increasingly large amplitude until they crash into the rods. As a results, the pair of positive rods acts as a high mass-to-charge ratio pass filter, transmitting only high masses. Conversely, along the y direction heavy ions (high m/e ratio) are destabilized by the DC voltage and finally encounter the two rods in the vertical direction. Therefore, the pair of negatively biased rods acts as a low mass-to-charge ratio pass filter, and the combined action of the quadrupole array results in a **band pass filter** (Fig. 4b). Specifically, it turns out that by suitably tuning the AC/DC ratio, only ions with a specific m/e ratio can pass through the quadrupole before being detected and properly amplified by, e.g., a secondary electron multiplier (SEM).

Note that the sample and the QMS are both mounted in an evacuated vessel kept under ultra-high-vacuum (UHV) conditions, therefore an essential prerequisite is that the pumping speed ensured by the pumping equipment is sufficiently high to prevent re-adsorption of desorbed species onto the surface. In this way, the signal monitored by the QMS can be assumed to be proportional to the number of desorbing particles.

The physics of desorption processes is usually described in terms of a Arrhenius-type behaviour, with the rate of desorption obeying the so-called *Polanyi-Wigner equation*:

$$-\frac{dn}{dt} = \nu_x \; n^x(t) \; e^{-\frac{E_{\text{des}}}{k_B T}} \tag{1}$$

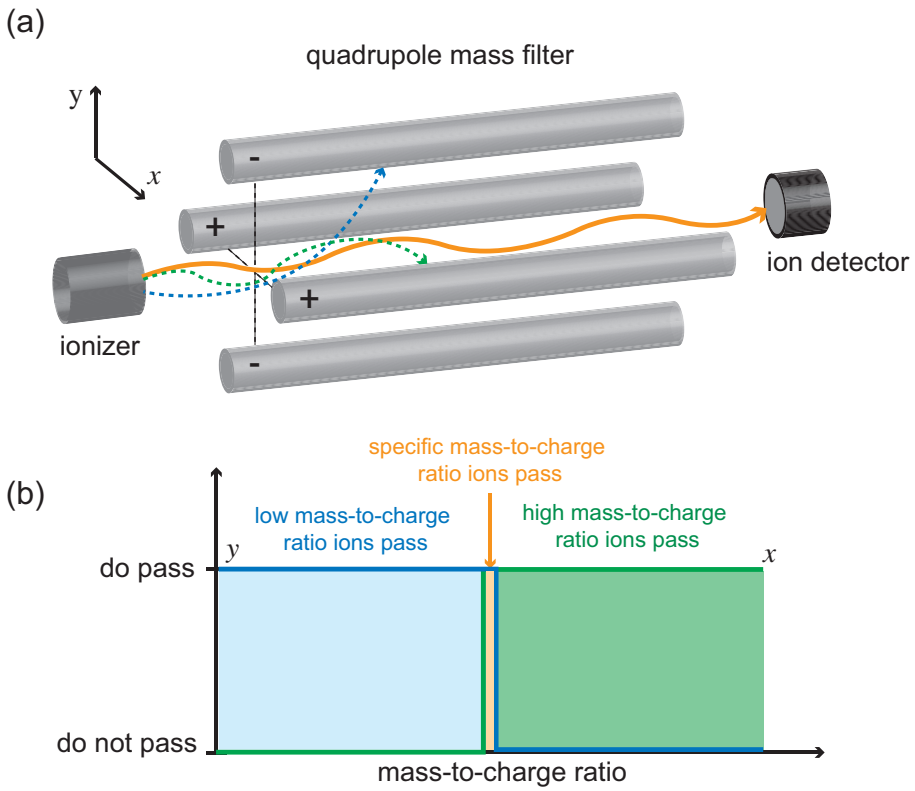

Figure 4: (a) Schematics of a Quadrupole Mass Spectrometer (QMS). The principal components are indicated. In the quadrupole mass filter the two sets of opposite rods are biased at the potential $\pm[\mathrm{U_{DC}} + \mathrm{V_{AC}} \cdot \cos(\omega \mathrm{t})]$ respectively. (b) Simplified diagram illustrating the filtering action of the QMS: only ions with a specific mass-to-charge ratio can pass through the array of quadrupole rods.

or equivalently:

$$-\frac{dn}{dT} = \frac{\nu_x \, n^x}{\beta} \, e^{-\frac{E_{\mathrm{des}}}{k_B T}} \tag{2}$$

In these equations, n denotes the surface concentration of the desorbing species, ν_x is a frequency factor (or *pre-exponential*), x accounts for the order of the desorption, and E_{des} is the activation energy (per molecule) for desorption, whereas k_B is the Boltzmann constant and β describes the linear heating rate. In the simplest cases, zero-, first- or second-order desorption take place ($x = 0,\ 1$ and 2 respectively):

- Zero-order desorption is often observed for thick molecular layers (so-called condensed *multilayers*). In this case, the supply of particles can be considered to be approximately unlimited and the desorption rate does not depend on the particle concentration n or, in other terms, on the molecular coverage $\Theta = n/n_{\mathrm{surf}}$[1](cf. Eq. 2 with $x = 0$). TPD spectra (QMS signal vs. T) recorded at different initial coverage display, therefore, a common leading edge, which is defined by the temperature at which the desorption sets in. However, when eventually all molecules have desorbed, a sudden drop following a desorption maximum is observed in the TPD spectrum. It also follows that at a given heating rate the temperature of the desorption maximum, T_m, moves to higher values as the initial coverage is increased. In addition, when the coverage drops the order of the process can change to $x > 0$, yielding an additional peak in the spectrum.

[1]Here n_{surf} is the density of surface unit cells; $\Theta = 1$ thus corresponds to a surface density of an adsorbed particle per surface unit cell and is conventionally referred to as a *monolayer*.

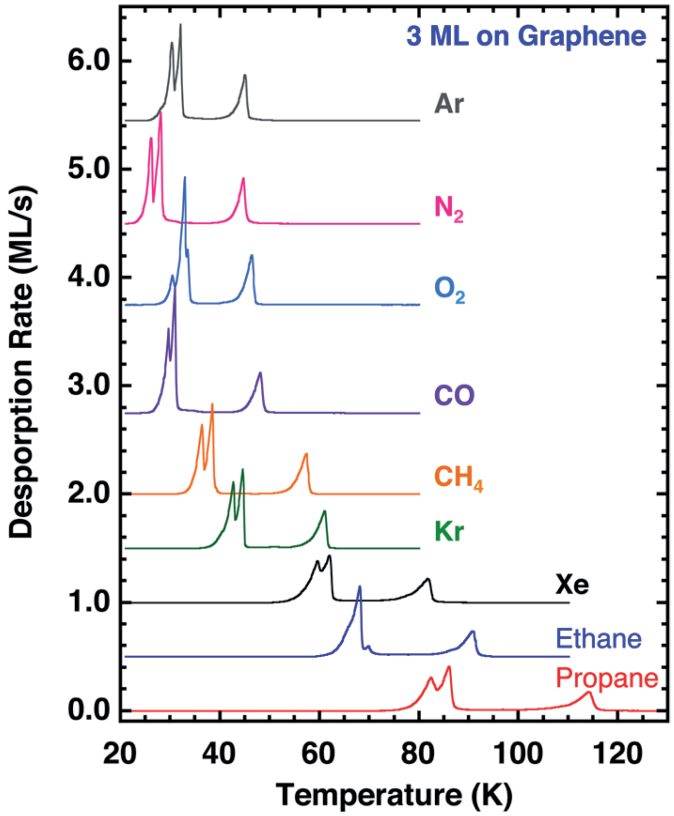

Figure 5: Examples of TPD spectra taken from Ref. [8]. The TPD spectra pertain to 3 monolayers (3 ML) of Ar, N_2, O_2, CO, CH_4, Kr, Xe, ethane and propane, respectively, adsorbed on graphene. All adsorbates were deposited at 25 K and heated at 1.0 K/s. The spectra are offset vertically for clarity of display.

- In a first-order desorption ($x = 1$), the desorption rate of the particles is directly proportional to the surface concentration n (see eq. 2). The maximum in the desorption rate can be found by imposing the condition that its first derivative with respect to T vanishes,[2] yielding [4]:

$$\frac{E_{\mathrm{des}}}{k_B T_m^2} = \frac{\nu_1}{\beta}\, e^{-\frac{E_{\mathrm{des}}}{k_B T_m}} \tag{3}$$

  This equation is independent of n, thus implying that T_m does not depend on the surface coverage. Therefore, a first-order desorption peak in a TPD spectrum will display its maximum at the same temperature regardless of the initial coverage.[3] Note, however, that adsorption of particles in distinct sites of the surface and/or multiple binding states can lead to multiple-peak spectra, often rendering the interpretation more elaborate.

- In the case of second-order kinetics ($x = 2$), such that observed for recombinative desorption of adsorbed H atoms into dihydrogen, the condition for a maximum in the desorption rate corresponds to [4, 5]:

$$\frac{E_{\mathrm{des}}}{k_B T_m^2} = \frac{\nu_2 \cdot n_0}{\beta}\, e^{-\frac{E_{\mathrm{des}}}{k_B T_m}} \tag{4}$$

[2] For the sake of simplicity it is often implicitly assumed that in eq. 2 E_{des} and ν_x do not depend on n

[3] It is worth noting that this conclusion is strictly true only if E_{des} and ν_x are not coverage-dependent.

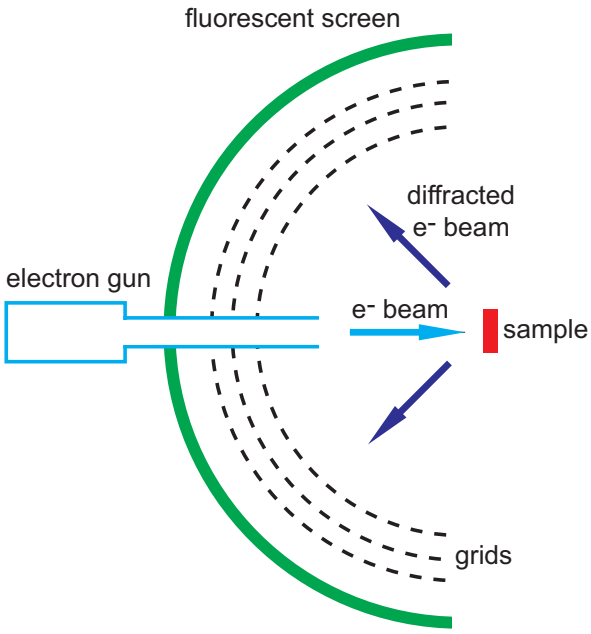

Figure 6: Schematics of a typical LEED set-up. The principal components are indicated.

In fact, it turns out that $2n(T_m) = n_0$ with n_0 initial surface concentration of particles. Eq. 4 shows that in contrast with first-order desorption, the temperature T_m of the desorption maximum is a function of the initial concentration n_0. As a consequence, T_m shifts to lower temperature as the initial coverage increases. This effect can be roughly rationalized in terms of the increased probability for two particles to find each other and recombine into the desorption product.

The previous equations may allow, under favourable conditions, the determination of important parameters influencing the reaction kinetics, such as the frequency factor and the activation energy for thesorption. However, in practice, desorption spectra from molecular adsorbates on surfaces can be rather complex, depending on the degree of complexity of the adsorbate itself. Hence, a quantitative analysis is generally not straightforward and may rely on different approximations. For a more detailed discussion the reader is referred to, e.g., Refs. [4, 5, 6, 7]. Exemplary TPD spectra are reported in Fig. 5.

3.2 Low-energy Electron Diffraction

Low-energy electron diffraction (LEED) is one of the most important techniques for surface analysis and has become a standard tool in many laboratories. It is primarily used to assess the crystallographic quality of surfaces, and in the presence of adsorbates it is widely employed to study the formation of long-range ordered superstructures, as it gives access in a simple way to the symmetry, size and rotational alignment of the adsorbate unit cell relative to the surface unit cell of the underlying substrate.

In a typical LEED experiment, a collimated beam of monochromatic low-energy electrons (i.e., electrons with energy E_{kin} in the range $10 - 300$ eV) impinges on the surface of a sample at normal incidence, and the elastically backscattered electrons are detected on a fluorescent screen (Fig. 6). The electrons are emitted by an electron gun, which consists of a cathode (e.g., a W or a LaB_6 filament) and a set of focusing lenses. The LEED pattern observed on the screen intrinsically reflects the wave-particle duality of matter: the coherent interference of the de Broglie electron waves backscattered by the surface atoms generates a discrete set of diffraction spots (the so-called *Bragg spots*), which is distinctive

of the periodicity and symmetry of the investigated system. Solely elastically backscattered electrons contribute to the diffraction pattern, and due to the strong electron-matter interaction this implies that only the scattering from the first few layers underneath the sample surface will determine the LEED signal, thus conveying high surface-sensitivity to the technique. To single out exclusively the elastically scattered electrons and reduce the background intensity, the retarding field of a set of grids placed in front of the fluorescent screen is used to filter out inelastically scattered electrons.

The condition for constructive interference upon diffraction of the de Broglie electron waves with wavelength $\lambda = h/p = h/\sqrt{2m_e E_{\text{kin}}}$ is given by the well-known Laue condition, which describes − for instance − the diffraction of X-rays from a crystal. This is written as:

$$\mathbf{k} - \mathbf{k_0} = \mathbf{G} \tag{5}$$

where $\mathbf{k_0}$ and $\mathbf{k}$ are the incident and scattered wavevectors, respectively, and $\mathbf{G}$ is a reciprocal lattice vector of the periodic system from which the electron waves are scattered. As mentioned, the penetration and escape depth of the electrons is of the order of few atomic layers, therefore the elastic scattering only occurs from the two-dimensional surface structure, and the Laue condition takes the form [5]:

$$\mathbf{k}_{||} - \mathbf{k}_{||,\mathbf{0}} = \mathbf{G}_{||} \tag{6}$$

where $\mathbf{k}_{||,\mathbf{0}}$ and $\mathbf{k}_{||}$ are the electron wavevector components parallel to the surface, and $\mathbf{G}_{||}$ is a generic vector of the two-dimensional (2-D) reciprocal lattice of the surface. Specifically, $\mathbf{G}_{||}$ can be written as:

$$\mathbf{G}_{||} = h\mathbf{a}^* + k\mathbf{b}^* \tag{7}$$

with $h,\ k$ integers and $\mathbf{a}^*$, $\mathbf{b}^*$ indicating the primitive vectors of the 2-D reciprocal lattice. In turn, denoting the primitive vectors of the 2-D real lattice associated to the surface as $\mathbf{a}$ and $\mathbf{b}$, it is [5]:

$$\mathbf{a}^* = 2\pi\ \frac{\mathbf{b} \times \mathbf{n}}{A} \tag{8}$$

$$\mathbf{b}^* = 2\pi\ \frac{\mathbf{n} \times \mathbf{a}}{A} \tag{9}$$

$$A = \mathbf{a} \cdot (\mathbf{b} \times \mathbf{n}) \tag{10}$$

where $\mathbf{n}$ is a unit vector normal to the surface, and A yields the area of the surface primitive cell in the real space.

The so-called *Ewald construction* is often used to illustrate in a pictorial way under which conditions Eq. 5 is fulfilled and to rationalize changes in the discrete LEED pattern. In Fig. 7a the Ewald sphere (circle) is drawn. It has radius equal to $|\mathbf{k_0}|$ and passes through the origin of the reciprocal lattice. The elastic scattering condition ($|\mathbf{k}| = |\mathbf{k_0}|$) implies that the final wavevector must lie with his tip on the Ewald sphere, having imposed that the incident wavevector has its center on the Ewald sphere and its tip in the origin of the reciprocal space. A diffraction peak is observed whenever the associated reciprocal lattice vector intersects the Ewald sphere, as this corresponds to meet the condition of Eq. 5. Therefore, only a discrete subset of Bragg spots is observed at a certain wavelength and incidence geometry. In the 2-D case, the lattice constant along the surface normal in real space has to be assumed to be infinite (the electrons being predominantly scattered by the two-dimensional surface structure, such that perpendicularly to the surface the periodicity is broken): hence, in that direction the reciprocal lattice points are very closely spaced and form (so-called) *reciprocal lattice rods*. Considering a cut of the Ewald sphere perpendicular to the surface, one then obtains the diagram of Fig. 7b. A spot in the LEED pattern is observed if and only if the difference in the parallel components of the

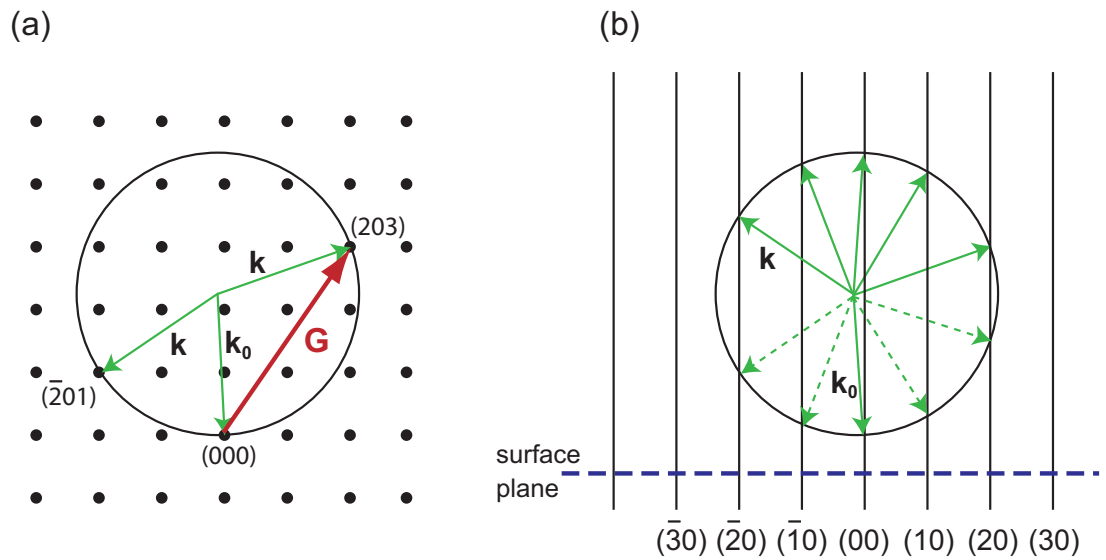

Figure 7: (a) Ewald sphere construction for the 3-dimensional (bulk) case. The incident wavevector is denoted as $\mathbf{k_0}$ and possible scattered wavevectors are indicated with $\mathbf{k}$; the reciprocal lattice vectors $\mathbf{G}$ associated with the Bragg reflections are decomposed into integer components (hkl). (b) Ewald sphere construction for the 2-dimensional (surface) case. Reciprocal lattice rods normal to the surface plane are drawn, and the intersections with the Ewald sphere (circle) generate Bragg reflections labelled by two integers. The dashed scattered wavevectors propagate into the solid and therefore cannot be observed. As the modulus of the wavevector increases with the electron energy, at higher energies more reflections are recorded on the fluorescent screen.

incident and scattered wavevectors results in a momentum transfer $\mathbf{\Delta k}_{||} = \mathbf{k}_{||} - \mathbf{k}_{||,\mathbf{0}}$[4] that equals a multiple of the reciprocal lattice constant of the surface, namely whenever the Ewald circle intersects a reciprocal lattice rod. The Bragg spots on the fluorescent screen are thus observed along the directions of $\mathbf{k}$. The resulting LEED pattern directly reflects the structure and symmetry of the reciprocal lattice of the surface or superstructure and therefore, *via* Eqs. 8−10, conclusions regarding the ordering in the real space can be drawn.

An illustrative example of LEED pattern for a surface superstructure is reported in Fig. 8, see panel (a), where also the linking between real and reciprocal space is sketched in panels (b) and (c).

4 Experimental set-up

The experimental set-up that will be used for the experiment is schematically depicted in Fig. 9 and is based on an UHV chamber on which the quadrupole mass spectrometer for TPD analysis, a commercial LEED apparatus (SPECTALEED, Omicron NanoTechnology GmbH) and all ancillary facilities for sample insertion, preparation and manipulation are mounted.

4.1 The vacuum system

The UHV chamber is operated at a base pressure of about 3×10^{-10} mbar (3×10^{-8} Pa). Such a low pressure is necessary to ensure that atomically clean surfaces are maintained free of contaminants during the experiments. It is also necessary for the standard operation of the electron-based LEED apparatus and to avoid interference from residual gases during the desorption experiments. The chamber is pumped by a turbomolecular pump directly mounted inside the chamber and backed by a suitable roughing pump. The UHV regime

[4]Note that at normal incidence, as commoly employed in LEED, $k_{||,0} = 0$.

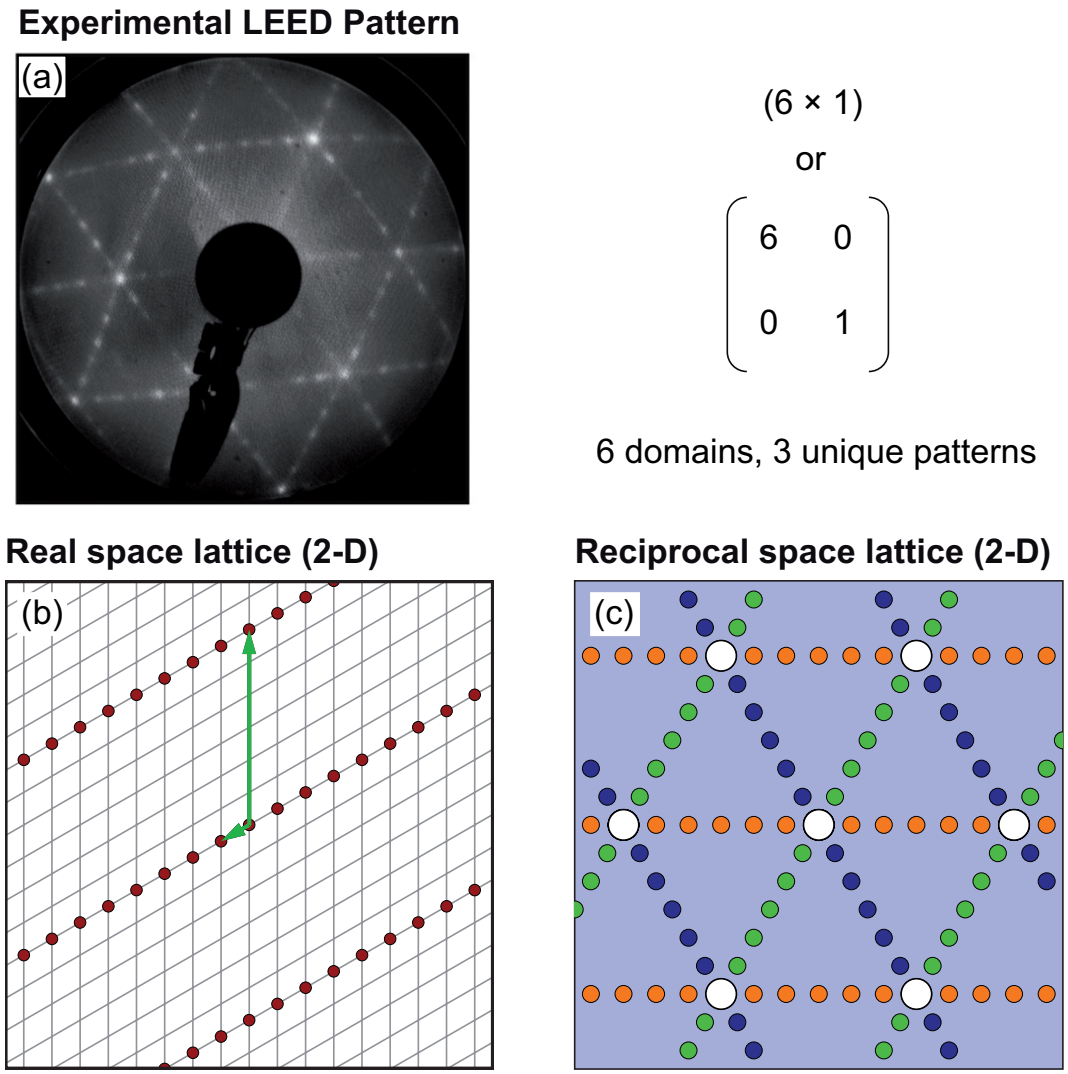

Figure 8: (a) Example of experimental LEED pattern for a single layer of Ni oxide grown on the threefold symmetric Rh(111) surface [9]. The characteristic streaked appearance signals a (6×1) superstructure, with its matrix notation given on the right with respect to the primitive vectors of the pristine Rh surface. (b) Real space representation of the 2-D (6×1) superstructure. The primitive vectors are drawn (green). (c) Simulated LEED pattern computed by using the LEEDpat4.2 software [10]. It arises from the superposition of three unique patterns, due to the 120° rotational symmetry and the mirror symmetry of the substrate (see 2b), leading to six possible adsorbate domains.

can only be reached after baking out the entire chamber for 24-36 hours at temperatures exceeding 160-180 °C. This procedure allows to eliminate residual molecules (predominantly water) adsorbed on the stainless steel walls of the chamber, which otherwise would be released at a low rate thus raising the residual pressure. A brief introduction to the UHV technology, instrumentation and related protocols can be found in Ref. [11].

4.2 Facilities

The quadrupole mass spectrometer and LEED optics are mounted on opposite sides of the experimental chamber. A Ru(0001) single crystal is fixed onto a sample holder which is mounted on a linear manipulator with four degrees of freedom; the latter allows not only translational motion along three orthogonal directions, parallel and perpendicular to the manipulator axis, but also rotation around such an axis, such that the sample surface can be easily brought to face different components inside the chamber.

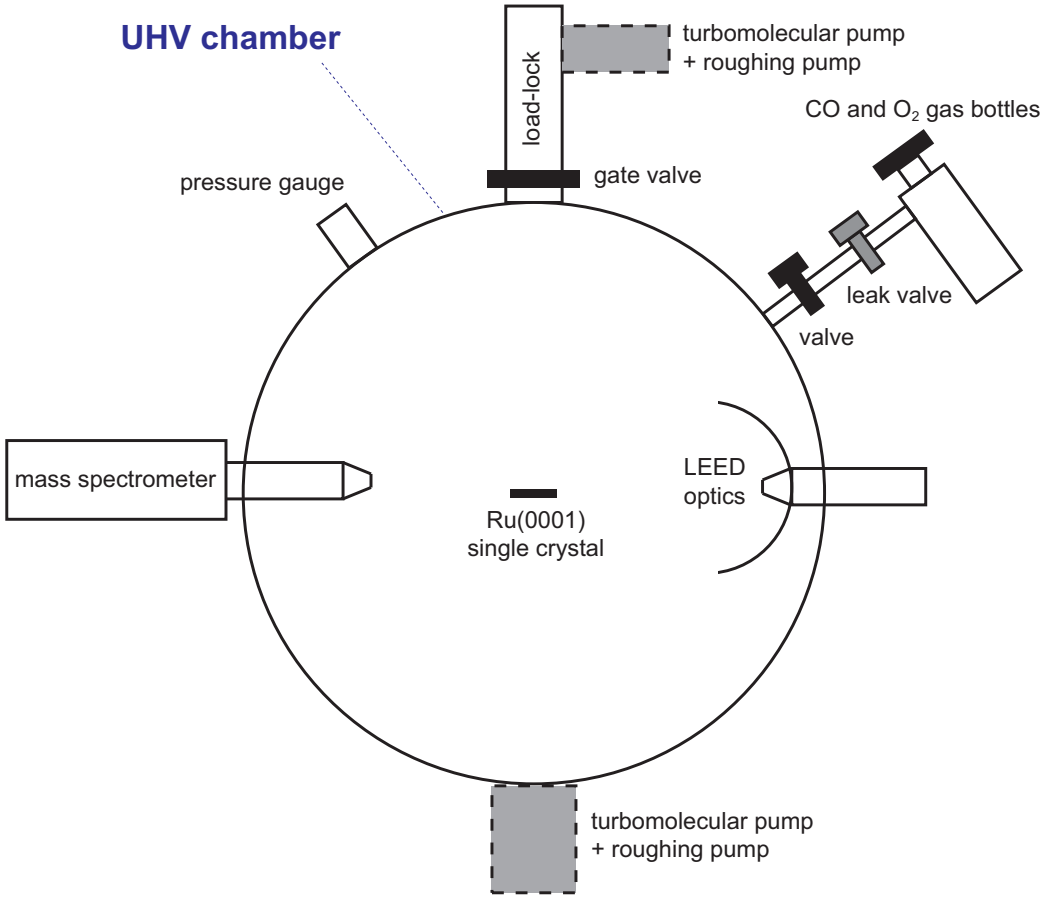

Figure 9: Side view of the UHV chamber used for the F-Praktikum experiment, on which the quadrupole mass spectrometer (left), the LEED optics (right), and all equipments required for pumping, UHV monitoring and surface preparation are mounted. The Ru(0001) single crystal is mounted onto a horizontal manipulator (not drawn) directed perpendicularly to the figure plane.

The sample can be heated up to ~ 1600 K *via* electron bombardment, with the electrons being supplied by a tungsten filament located behind the crystal and then accelerated against the back of the sample by a high voltage difference (up to 1 kV). The reaction of dioxygen (O_2) molecules with the Ru surface at elevated temperature is used to remove residual carbon present on the surface and thus to prepare a clean (1×1)-Ru(0001) surface free of contaminants.

The sample can also be cooled down to 80-100 K via a liquid nitrogen reservoir. During the TPD measurements the Ru crystal is then heated at a constant rate (typically, in the range $0.5 - 5$ K/s). The heating rate can be controlled by a home-made proportional-integral-derivative (PID) controller, and the temperature is monitored by a K-type thermocouple spot-welded onto an edge of the crystal.

Carbon monoxide (CO) molecules can be deposited onto the surface either at low temperature or at room temperature (300 K). The CO gas (as O_2 previously) can be let into the chamber in a controllable way through a high-precision leak valve, after filling a gas handling line installed before the valve. The partial CO pressure in the main chamber is monitored by means of a suitable hot-filament ionization gauge.

Finally, note that the Ru(0001) sample can be introduced into the chamber without breaking the vacuum employing a custom-built load-lock system (Fig. 9, top).

5 Important concepts

Before coming to the experiment, the following items should be checked and understood:

- Fundamental principles of TPD & LEED, main information that these techniques can yield.
- Basic understanding of adsorption phenomena.
- Basic concepts and working principles of the instrumentation involved.
- Make sure you have read the following instructions and if something is unclear discuss the issue with your advisor.
- What is the structure of a ruthenium crystal? Face-centred cubic (fcc) or hexagonal close-packed (hcp)? How does the symmetry of the (0001) surface look like?

6 Instructions for the experimental session

Subsequent steps will be tackled during the experiment, see below. The advisor will give you explanations and assist you.

A. Ru(0001) surface preparation

A clean Ru(0001) surface is the prerequisite for the CO adsorption. As elemental carbon is the intrinsic source of impurities embedded in a Ru bulk crystal, oxygen treatment is required to remove carbon contamination from the surface.

1. Cool down the flowing cryostat of the manipulator with liquid nitrogen (LN_2).
2. Drive the manipulator head away from the LEED apparatus and close to a viewport for a better visualization.
3. Heat the Ru(0001) crystal to 1570 K by electron-beam bombardment at 1 kV and stay at 1570 K for 20 seconds. Here you will be operating the heating control unit manually. Check the colour of the sample!
4. After stopping the heating, introduce dioxygen through the designated leak valve during the cooling from 1200 to 500 K and keep the partial O_2 pressure at 1×10^{-6} mbar.
5. Repeat steps 3 and 4 for three times.
6. To remove residual adsorbed CO molecules and O adatoms, which form on the surface during the oxygen treatment, the Ru(0001) crystal needs to be flashed to 1570 K for additional three times in vacuum (i.e., without O_2).

B. Deposition of CO molecules on Ru(0001)

7. Move the Ru(0001) crystal in front of the directional doser, which is connected to the CO gas line.
8. Keep the substrate temperature at 300 K, which helps to decrease the amount of CO adsorbed on the manipulator head.

9. Dose CO at a base pressure of 1×10^{-6} mbar in the experimental chamber for 60 seconds (this corresponds to a nominal *exposure* of 60 Langmuir; 1 Langmuir = 1.33×10^{-6} mbar·s) − note, however, that the effective exposure is larger, due to the higher local pressure close to the doser and sample. A full chemisorbed layer should be obtained under these conditions (*saturation coverage*).

C. LEED experiment

Different CO coverages, which can be obtained by annealing the sample to moderate temperatures (thus desorbing part of the CO molecules), correspond to different packing arrangements of the adsorbed CO molecules and distinct long-range periodicity. The symmetry as well as the orientation of the primitive vectors of the superstructures can be determined from the ordered electron diffraction patterns shown on the LEED screen.

10. Switch off the heating filament of the sample holder.

11. Position the sample in front of the LEED electron gun and rotate the manipulator to reach the geometry in which the electrons impinge at normal incidence to the sample surface.

12. Switch on the power supply driving the LEED optics. Set the screen voltage to 6 kV and increase slowly the filament current up to 1.26 A. Select an initial electron energy of 100 eV (sensitive to the first-order LEED spots).

13. Switch off all the lights in the laboratory and draw the curtains. Switch off the ionization gauge filament to suppress every possible source of light. If necessary cover each glass window in the chamber with a black cloth.

14. Fine-tune the crystal position and the electron energy to find the sharpest LEED spots on the screen.

15. Take photos of the relevant LEED patterns for each of the following annealing steps: 300 K, 365 K and 430 K. If possible, take the photos at various electron energies, but try to use similar electron energies for different superstructures, as later you might need to compare the LEED patterns to each other.

D. TPD experiment

In this part, TPD spectra of three samples with different CO coverages will be acquired and compared to each other to highlight differences in the evolution.

16. After the LEED experiment anneal the Ru(0001) crystal to 600 K to desorb residual CO molecules from the surface, and afterwards prepare a full CO single layer (the saturation coverage) at 200 K.

17. With the aid of the advisor, change the configuration of the LN_2 cooling from pipeline to bucket (to prevent temperature oscillations during the TPD scan, induced by unstable LN_2 flow rate).

18. Start the mass spectrometer.

19. Bring the sample into the position for TPD.

20. Start a TPD scan after choosing the default linear heating rate (which you will not change in the following scans). Temperature range: from 200 K to 650 K. The partial pressure of desorbing CO molecules is read by the computer program and plotted as a function of time (later converted into the temperature scale.

21. Display the TPD spectrum with Igor Pro software.

22. Prepare another full layer and anneal it to 365 K and 433 K, respectively, for the next two samples.

23. Take TPD spectra of the samples according to steps 18-21.

24. Compare the resulting three TPD spectra and check the difference.

E. The effect of electron-beam damage on the CO layer

In this experiment, the effect of the electron beam on the CO adsorbed on Ru(0001) will be examined. You will find out that the bombardment with electrons of energy around 200 eV can cause C−O bond breaking in the adsorbed molecules. As a result, carbon and oxygen atoms from the dissociated CO molecules will accumulate on the Ru(0001) surface and rearrange themselves locally. A new superstructure is formed, which can be observed with LEED.

25. Prepare the 430 K phase that you have characterized by LEED before and move the sample into the LEED position.

26. Set the electron energy at 200 eV and keep the sample at 430 K under electron bombardment for 5 minutes.

27. Check the LEED pattern from the beam damaged area and compare it with the LEED pattern of an intact area by moving to a new place on the sample. What is the new periodicity?

7 How to write the report

The report contains six parts:

- **Abstract**: brief summary of the content and main achievement(s) of the report.
- **Introduction**: introduce the related research domain and goals of this experiment.
- **Experimental methods**:
    1. Describe the experimental set-up/apparatus, specifically what you have seen and used in the lab. A detailed presentation of the techniques is not needed, so please do not try and rephrase the explanations provided in this script.
    2. Describe the sample preparation procedure:
        a. Give details of the Ru(0001) surface cleaning procedure.
        b. How samples of different CO coverage are prepared.
        c. How the electron-beam induced CO dissociation is performed.
    3. Explain how LEED images are acquired (measuring geometry, electron energy, sample temperature ...).
    4. How TPD spectra are recorded (measuring geometry, temperature range, heating rate, background pressure in the UHV chamber ...).
- **Experimental results**:
    1. Display LEED pictures corresponding to different samples.
    2. Report the TPD curves for different measurements (different CO coverages), e.g. vertically stacked on the same plot.

- **Data analysis and discussion**:
    1. Analyse the LEED patterns (a more detailed description of the procedure and conventional LEED notations will be provided during the experimental session), and assign the registry and unit cell parameters for different CO (or O) superstructures/arrangements. The exercise in section 8 will be useful during your analysis.
    2. Interpret and compare the characteristics of the TPD spectra of differently prepared systems. What is the CO desorption order on Ru(0001)?
    3. Discuss the correlation between the LEED data with the TPD spectra of different coverage.
    4. Compare your results to the state-of-the-art knowledge on the CO/Ru(0001) system, in particular, search the scientific literature for work by D. Menzel and co-workers.
- **Conclusion**: give a short summary of the work you have done and what you have learnt, and summarize the amount of information you can extract from the measured data.

8 Exercise

By applying the definition given for the primitive vectors in the reciprocal space (Eqs. 8−10), show that the reciprocal lattice of a 2-D hexagonal lattice is also a hexagonal lattice, but it is rotated by 90°. What is the relationship between the sides of the two hexagons?

References

[1] J. L. F. Da Silva, C. Stampfl and M. Scheffler, *Adsorption of Xe Atoms on Metal Surfaces: New Insights from First-Principles Calculations*, Physical Review Letters **90**, 066104 (2003); doi:10.1103/PhysRevLett.90.066104.

[2] M. Smedh et al., *Vibrationally Resolved C 1s Photoemission from CO Absorbed on Rh(111): The Investigation of a New Chemically Shifted C 1s Component*, Surface Science **491**, 99 (2001); doi:10.1016/S0039-6028(01)01357-7.

[3] H. Lüth, *Solid Surfaces, Interfaces and Thin Films*, Springer-Verlag, Berlin Heidelberg, 2010 (5th Edition). Chapters 2 and 10.

[4] K. W. Kolasinski, *Surface Science − Foundations of Catalysis and Nanoscience*, Wiley, 2009 (2nd edition). Chapter 4.

[5] D. P. Woodruff and T. A. Delchar, *Modern Techniques of Surface Science*, Cambridge University Press, 1994. Chapters 2 and 5.

[6] D. A. King, *Thermal Desorption from Metal Surfaces: A Review*, Surface Science **47**, 384 (1975); doi:10.1016/0039-6028(75)90302-7.

[7] A. M. de Jong and J. W. Niemantsverdriet, *Thermal Desorption Analysis: Comparative Test of Ten Commonly Applied Procedures*, Surface Science **233**, 355 (1990); doi:10.1016/0039-6028(90)90649-S.

[8] R. S. Smith, R. A. May and B. D. Kay, *Desorption Kinetics of Ar, Kr, Xe, N_2, O_2, CO, Methane, Ethane, and Propane from Graphene and Amorphous Solid Water Surfaces*, The Journal of Physical Chemistry B, **120**, 1979 (2016); doi:10.1021/acs.jpcb.5b10033.

[9] L. Gragnaniello et al., *Surface Structure of Nickel Oxide Layers on a Rh(111) Surface*, Surface Science, **611**, 86 (2013); doi:10.1016/j.susc.2013.01.018.

[10] K. Hermann and M. A. V. Hove, *LEEDpat4 (LEED pattern analyzer)*, http://www.fhi-berlin.mpg.de/KHsoftware/LEEDpat/, Version 4.2 (December 2015).

[11] K. Oura, V. G. Lifshits, A. A. Saranin, A. V. Zotov and M. Katayama, *Surface Science – An Introduction*, Springer-Verlag, Berlin, 2010. Chapter 3.